Eur. Phys. J. C 52, 665–672 (2007)
DOI 10.1140/epjc/s10052-007-0396-2

THE EUROPEAN PHYSICAL JOURNAL C

Regular Article – Theoretical Physics

Signature of heavy charged Higgs boson at LHC in the 1 and 3 prong hadronic tau decay channels

M. Guchait[1,a], R. Kinnunen[2], D.P. Roy[3]

[1] Department of High Energy Physics, Tata Institute of Fundamental Research, Homi Bhabha Road, Mumbai-400005, India
[2] Helsinki Institute of Physics, Helsinki, Finland
[3] Homi Bhabha Centre for Science Education, Tata Institute of Fundamental Research, V.N. Purav Marg, Mumbai-400088, India

Received: 17 May 2007 / Revised version: 5 July 2007 /
Published online: 13 September 2007 –

Abstract. We have done a fast simulation analysis of the $H^{\pm}$ signal at LHC in 1 and 3 prong hadronic τ-jet channels along with a $t\bar{t}$ background. The τ polarization was effectively used to suppress the background in both channels. Combining this with appropriate cuts on p_{T} of the τ-jet, the missing E_{T} and the azimuthal angle between them reduces the background below the signal level. Consequently, one gets a viable $H^{\pm}$ signal up to a mass range of 600–700 GeV at moderate to large $\tan\beta$.

1 Introduction

The minimal supersymmetric standard model (MSSM) contains a pair of charged Higgs bosons $H^{\pm}$ along with three neutral ones. While it may be hard to distinguish any of the neutral Higgs bosons from that of the standard model, the $H^{\pm}$ carries the unambiguous hallmark of the MSSM Higgs sector. Therefore, it has an important role in the search of MSSM Higgs bosons at the large hadron collider (LHC). The leading order QCD process

$$gb \to tH^{\pm} + \mathrm{h.c.} \tag{1}$$

gives a sizable production cross-section for a heavy $H^{\pm}$ at LHC. However, its dominant decay mode, $H^{\pm} \to t\bar{b}$, suffers from a large QCD background [1]. A more promising signature comes from its leading sub-dominant decay mode,

$$H^{\pm} \to \tau^{\pm}\nu_{\tau}\,, \tag{2}$$

which accounts for the branching fraction of $\gtrsim 10\%$ in the moderate to large $\tan\beta(\gtrsim 10)$ region. Moreover, one can enhance this signal over the SM background from

$$W^{\pm} \to \tau^{\pm}\nu_{\tau} \tag{3}$$

by exploiting the opposite polarizations of τ i.e. $P_{\tau} = +1$ and -1 from the signal (2) and background (3), respectively. This was shown to give a viable signature for a heavy $H^{\pm}$ boson at LHC in its 1 prong hadronic τ decay channel [2]. In particular, the signal to background ratio was shown to be enhanced significantly by requiring the charged prong to carry $> 80\%$ of the visible τ-jet energy.

The work of [2] was based on a parton level Monte Carlo simulation for the $H^{\pm} \to \tau^{\pm}\nu_{\tau}$ signal (2) and the $W^{\pm} \to \tau^{\pm}\nu_{\tau}$ background (3), followed by a simple hadronic τ decay code via

$$\tau \to \pi^{\pm}\nu(12.5\%), \rho^{\pm}\nu(26\%), a_1^{\pm}\nu(15\%)\,. \tag{4}$$

The $a_1^{\pm}$ mode contributes half and half to the 1 prong ($\pi^{\pm}\pi^0\pi^0$) and 3 prong ($\pi^{\pm}\pi^{\pm}\pi^{\mp}$) channels. So the three mesons of (4) account for over 90% of the 1 prong hadronic decay branching ratio (BR) of $\tau(\simeq 50\%)$ [3]. A more exact analysis was done in [4] following the same procedure, where the signal (2) and background (3) were simulated using the PYTHIA Monte Carlo (MC) event generator [7] along with the fast CMSJET package for detector simulation [8]. A similar analysis was also done by members of the ATLAS collaboration [9]. In this paper we investigate the signal (2) and background (3) in both 1 and 3 prong hadronic decay channels of τ along the lines of [4].

However, we have used the TAUOLA package [10, 11] for hadronic τ decay unlike [4], which had used the simple decay code of [2] via (4). The two τ decay programs give very similar results. But the TAUOLA package is more exact, since it includes the small non-resonant contribution to hadronic τ decay. Besides this, it is the first investigation of this process including both 1 and 3 prong hadronic decay channels of τ.

2 τ polarization

It is easy to understand the effect of τ polarization (P_{τ}) on its 1 prong hadronic decay via the dominant contributions

[a] e-mail: guchait@tifr.res.in

of (4). The center of mass angular distributions of τ into π or a vector meson $v(=\rho, a_1)$ is simply given in terms of its polarization as

$$\frac{1}{\Gamma_\pi}\frac{\mathrm{d}\Gamma_\pi}{\mathrm{d}\cos\theta} = \frac{1}{2}(1+P_\tau\cos\theta)\,,$$
$$\frac{1}{\Gamma_v}\frac{\mathrm{d}\Gamma_{v\mathrm{L,T}}}{\mathrm{d}\cos\theta} = \frac{\frac{1}{2}m_\tau^2, m_v^2}{m_\tau^2+2m_v^2}(1\pm P_\tau\cos\theta)\,, \qquad (5)$$

where L, T denote the longitudinal and transverse polarization states of the vector meson. This angle is related to the fraction x of the τ lab momentum carried by the meson, i.e. the (visible) τ-jet momentum via

$$x = \frac{1}{2}(1+\cos\theta) + \frac{m_{\pi,v}^2}{2m_\tau^2}(1-\cos\theta)\,. \qquad (6)$$

It is clear from (5) and (6) that the signal ($P_\tau = +1$) has a harder τ-jet than the background ($P_\tau = -1$) for the π, ρ_L and $a_{1\mathrm{L}}$ contributions; but it is the opposite for the ρ_T and $a_{1\mathrm{T}}$ contributions. Now the transverse ρ and a_1 decays favor even sharing of the momentum among the decay pions, while the longitudinal ρ and a_1 decays favor uneven distributions, where the charged pion carries either very little or most of the momentum. Thus requiring the $\pi^\pm$ to carry $\gtrsim 80\%$ of the τ-jet momentum,

$$R_1 = \frac{p_{\pi^\pm}}{p_{\tau\text{-jet}}} \gtrsim 0.8\,, \qquad (7)$$

retains about half the longitudinal ρ along with the pion but very little of the transverse contributions. This cut suppresses not only the $W\to\tau\nu$ background, but also the fake τ background to the 1 prong hadronic decay channel from QCD jets.

The 3 prong hadronic decay accounts for about 15% of the τ decay, of which two-third (10%) comes from

$$\tau \to \pi^\pm\pi^\pm\pi^\mp\nu \qquad (8)$$

without any accompanying π^0. We shall consider only this 3 prong decay channel, which can be separated by either matching the tracker momentum of the τ-jet with the calorimetric energy deposit or by a veto on accompanying $\pi^0\to 2\gamma$ in the electromagnetic calorimeter (EM). This effectively suppresses the fake τ background from QCD jets, while retaining two-third of the genuine τ events. As mentioned above three-fourth of the 3 prong decay (8) comes from the a_1 contribution. Thus one can again enhance the $a_{1\mathrm{L}}$ contribution by imposing a cut on the fractional τ-jet momentum carried by the like-sign pair, i.e.

$$R_3 = \frac{p_{\pi^\pm\pi^\pm}}{p_{\tau\text{-jet}}} \neq 0.2{-}{-}0.8\,. \qquad (9)$$

We shall see that this cut favors the ($P_\tau = +1$) signal over the ($P_\tau = -1$) background significantly even after including the non-resonant contribution to (8). Note that the like-sign pion pair in the 3 prong ($\pi^\pm\pi^\pm\pi^\mp$) decay of a_1 is analogous to the neutral pion pair in its 1 prong ($\pi^0\pi^0\pi^\pm$) decay, i.e. R_3 corresponds to $1-R_1$ for the a_1 channel.

3 Signal and background

We have computed the $H^\pm$ signal from the leading order QCD process (1) using PYTHIA [7]. For simplicity we have used a common renormalization and factorization scale $\mu_\mathrm{R} = \mu_\mathrm{F} = \sqrt{\hat{s}}$. The resulting $H^\pm$ cross-section has been enhanced by a K factor of 1.5 to account for the higher order corrections following [12–14].[1] Alternatively, one could choose a smaller scale and correspondingly a smaller K factor [16]. Note that the $H^\pm$ Yukawa coupling of the signal process (1) is estimated using the running quark masses $m_t(\mu_\mathrm{R})$ and $m_b(\mu_\mathrm{R})$. Then it is followed by the hadronic decay of the top, $t\to bqq'$, along with the $H^\pm\to\tau^\pm\nu$ decay of (2). Finally, the hadronic decay of τ is simulated using TAUOLA [10, 11]. Thus the final state consists of at least four hard jets, including the τ-jet, along with a large missing E_T ($\not\!\!E_\mathrm{T}$). These events are expected to be triggered by a multi-jet trigger along with a higher level τ trigger with a high trigger efficiency of 90% at CMS [4].[2] The jets and the $\not\!\!E_\mathrm{T}$ are reconstructed with the fast CMS detector response simulation package CMSJET [8]. The program contains the detector resolution and the main cracks and inefficiencies.

The background was computed from the leading order $t\bar{t}$ production process using $\mu_\mathrm{R} = \mu_\mathrm{F} = \sqrt{\hat{s}}$ and multiplying the resulting cross-section with the appropriate K factor 1.3 [17], where $\sqrt{\hat{s}}$ is the center of mass energy in the partonic center of mass frame. This is followed by the hadronic decay of one top, $t\to bqq'$, while the other decay is via $t\to bW\to b\tau\nu$. We do not consider the other contributions to the background of (3) coming from $W+$multijet production, since they can be effectively suppressed by the reconstructions of the hadronic top mass and b-tagging [4]. Note however that the same polarization cut suppresses this $W+$multijet background as much as the $t\bar{t}$ background.

The τ identification is based on the narrowness of the τ-jet. To implement this we define a narrow signal cone of size $\Delta R_\mathrm{S} = 0.1$ and an isolation cone of size $\Delta R_\mathrm{I} = 0.4$ around the calorimetric jet axis, where ΔR is defined via the azimuthal angle and the pseudo-rapidity by

$$\Delta R = \sqrt{\Delta\phi^2+\Delta\eta^2}\,. \qquad (10)$$

We require 1 or 3 charged tracks inside the signal cone, with $|\eta|<2.5$ and $p_\mathrm{T}>3$ GeV for the hardest track, the former corresponding to the pseudo-rapidity coverage of the tracker. We further require that there are no other charged tracks with $p_\mathrm{T}>1$ GeV inside the isolation cone to ensure tracker isolation [4]. This was shown to be adequate to suppress the fake τ-jet background to the $W\to\tau\nu$ events of

[1] It has been recently suggested that still higher order corrections from the soft gluon threshold effect would enhance the K factor further by $\sim 20\%$ [15]. This has not been included, however, in our estimate of the signal.

[2] This trigger efficiency falls to 63%–64% in a full simulation[5, 6]. We have not included it in this work, however, since it is based on a fast simulation. Its effect will be to rescale the size of signal and background shown in Tables 1 and 2 as well as Figs. 1–7 by two-third. Correspondingly, the discovery limits of $\tan\beta$ in Fig. 8 will increase by 25%.

the CDF experiment in the 1 prong channel but not in the 3 prong channel [18, 19]. In the latter case one has to combine the tracker isolation with the requirements of narrow width and small invariant mass(< 1.8 GeV) of the τ-jet candidate using the calorimeter information to suppress the fake τ-jet background [18–21], which is beyond the scope of the present work. Note however that in the high-p_{T} range of our interest ($\gtrsim 100$ GeV), the 3 prong τ-jet is expected to be tagged by the secondary vertex [21]. Moreover, we are interested in a sub-sample of 3 prong τ-jets, without accompanying π^0s, for which the fake background is relatively small, as we shall see below.

We ensure the absence of π^0s by requiring the energy of the 3 charged tracks measured in the tracker to match with the calorimetric energy deposit of the τ-jet within the calorimetric energy resolution, i.e.

$$\Delta E = |E_{\mathrm{trk}}^{\mathrm{tot}} - E_{\mathrm{cal}}^{\mathrm{tot}}| < 10\,\mathrm{GeV}\,. \tag{11}$$

With this cut the τ-jet identified by the tracker matches well with the actual τ-jet of the event generator. Therefore, we shall use the tracker identification of the τ-jet in both 1 and 3 prong channels.

In our simulation, as a basic set of selection cuts for jet reconstruction, we apply

$$p_{\mathrm{T}}^{\mathrm{j}} > 20\,\mathrm{GeV}\,, \quad |\eta^{\mathrm{j}}| < 4.5\,, \tag{12}$$

for all jets, the latter corresponding to the pseudo-rapidity coverage of the calorimeter. We require a minimum separation of

$$\Delta R > 0.5 \tag{13}$$

between the jets. The missing E_{T} arising mainly due to the presence of ν_τ accompanied by the τ lepton, is reconstructed using the calorimetric information, and we set a minimum cut of

$$\not{E}_{\mathrm{T}} > 30\,\mathrm{GeV}\,. \tag{14}$$

The $\not{E}_{\mathrm{T}}$ is expected to be large for the signal as it originates mainly from the massive $H^{\pm} \to \tau\nu$ decay, whereas in the case of the background it comes from a relatively light $W \to \tau\nu$ decay.

In Fig. 1 we show the distribution of p_{T} of τ-jet ($p_{\mathrm{T}}^{\tau\text{-jet}}$) for the signal in the upper panel along with the background from $t\bar{t}$ in the lower panel. These distributions are subject to only the basic selection cuts of (11)–(14) and are normalized for an integrated luminosity of $\mathcal{L} = 100\,\mathrm{fb}^{-1}$. The signals are shown for two masses of $H^{\pm}$, $m_{H^{\pm}} = 300$ and 600 GeV, for $\tan\beta = 40$. Evidently, the higher the mass of $H^{\pm}$, the harder are the τ-jets. Notice that the signal cross-section is several orders of magnitude less than the background even for $p_{\mathrm{T}}^{\tau\text{-jet}} > 100$ GeV.

In Fig. 2 we demonstrate the distribution in R_1 (7) for the 1 prong decay channel of the τ-jet for both signal and background with $p_{\mathrm{T}}^{\tau\text{-jet}} > 100$ GeV. The spillover of the distribution to the $R_1 > 1$ region reflects the 15%–20% uncertainty in the calorimetric energy measurement of the τ-jet.

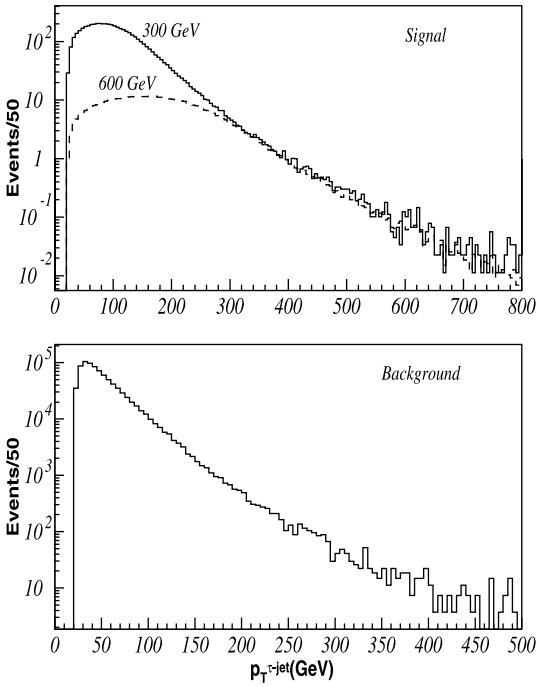

Fig. 1. The number of events are shown against p_{T} of τ-jets for signal and background processes for an integrated luminosity $\mathcal{L} = 100\,\mathrm{fb}^{-1}$ and subject to $p_{\mathrm{T}}^{\tau\text{-jet}} > 20$ GeV and $|\eta_{\tau\text{-jet}}| < 2.5$ cuts. The mass of charged Higgs and $\tan\beta$ are set to $m_{H^{\pm}} =$ 300 and 600 GeV and $\tan\beta = 40$

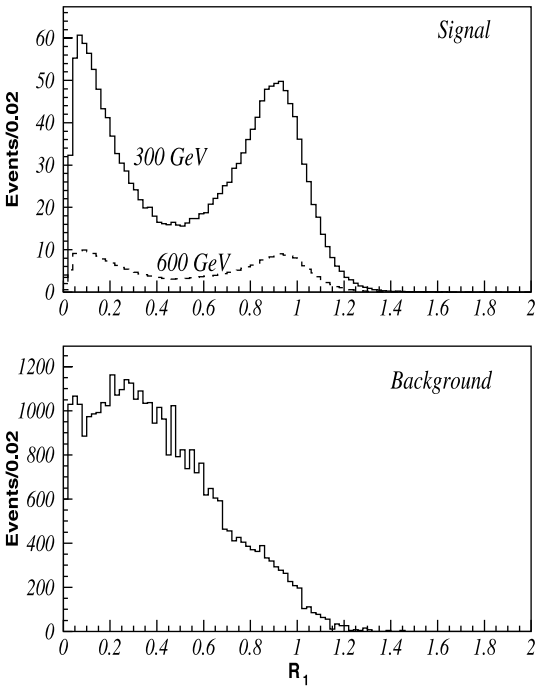

Fig. 2. The number of events are plotted against the fraction of τ-jet momentum carried by the charged prong R_1 for the 1 prong decay channel of the τ-jet for signal and background processes. Both distributions are subject to $p_{\mathrm{T}}^{\tau\text{-jet}} > 100$ GeV and $|\eta_{\tau\text{-jet}}| < 2.5$ cuts.The masses of charged Higgs and $\tan\beta$ are same as in Fig. 1

As discussed above, for the signal process where $P_\tau = +1$, peaks occur at the two ends because of the uneven sharing of energy between pions, while in the case of the background, for which $P_\tau = -1$, a peak occurs at the middle due to the almost equal sharing of energy between pions. Note that at the large R_1 end of the distributions the dominant contribution comes from $\rho_{\rm L}$ and π channels. Therefore, a cut like $R_1 > 0.8$ leads to a very large suppression of the background while retaining almost half of the signal events. Note that one would in any case require a reasonably hard charged track, corresponding to $R_1 \gtrsim 0.3$, for effective τ identification and rejection of the QCD jet background [20]. So extending this cut to $R_1 > 0.8$ costs very little to the signal, while it effectively suppresses the $P_\tau = -1$ background. For 3 prong decay of τ-jets we present the R_3 distribution in Fig. 3 for both signal and background, where R_3 is defined by (9). We have shown the distribution for two values of the $H^\pm$ mass as before. As mentioned above, the like-sign pair of πs plays the same role as the π^0 pair in the case of 1 prong decay channel of τ-jet via a_1, i.e. the $\pi^0\pi^0\pi^\pm$ channel. Hence, the like-sign pion pair carries either very little or most of the τ-jet energy for the signal ($P_\tau = +1$), while it carries roughly two-third of the τ-jet energy for the background ($P_\tau = -1$). Consequently, selecting events in the region $R_3 < 0.2$ and $R_3 > 0.8$ helps to suppress the background. We found that the efficiency due to this selection cut is about 55% for the signal and 35% for the background. Note that there is no constraint on R_3 for τ identification unlike the 1 prong channel. We would like to mention here that to a first approximation the choices of R_1 and R_3 cuts appear to us the best choices, but admittedly we have not done any numerical optimization.

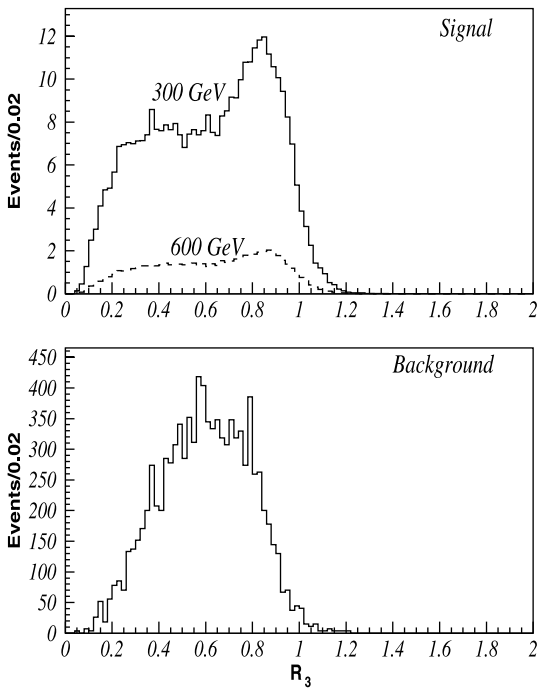

Fig. 3. Same as in Fig. 2, but against the fraction of τ-jet momentum carried by the like-sign pair (R_3) for the 3 prong τ-jet channel

Since the $H^\pm$ production (1) is accompanied by a top quark, it is useful to reconstruct the top quark mass. We perform the W and top mass reconstructions from hadronic decay modes by requiring at least three reconstructed jets in addition to a single τ-jet. For the W mass reconstruction we require the invariant mass of two jets to be

$$m_{\rm jj}^{\rm rec} = m_W \pm 15\,{\rm GeV} \tag{15}$$

and the corresponding W momenta are obtained out of these jet momenta. In case of several pairs satisfying this mass band, the pair having an invariant mass closest to m_W is chosen. The top mass reconstruction is performed using this pair and one of the remaining jets and demanding

$$m_{W{\rm j}}^{\rm rec} = m_t \pm 30\,{\rm GeV}\,. \tag{16}$$

Notice here that we have not done any kind of b-tagging.[3] However, to take care of b-tagging we multiply the signal and background cross-section by a b-tagging efficiency (ϵ_b) factor 0.5 [4]. This includes the loss of efficiency due to the reduced coverage of $|\eta| < 2.5$ for this jet. Though the $t\bar{t}$ background has two b-jets, one still gets an efficiency factor $2 \times 0.5 \times (1 - 0.5) = 0.5$ by requiring only one b-tag.

We have also investigated the relative azimuthal opening angle in the transverse plane between τ-jet and the $\not{E}_{\rm T}$ vector, which is also connected with the transverse mass, via

$$m_{\rm T} = \sqrt{2p_{\rm T}^{\tau\text{-jet}} \not{E}_{\rm T} \left(1 - \cos\Delta\phi(\tau\text{-jet}, \not{E}_{\rm T})\right)}\,. \tag{17}$$

Since in the signal process (2) both τ-jet and $\not{E}_{\rm T}$ are originating from a comparatively massive $H^\pm$ particle, leading to harder τ-jet and missing momentum, it is expected that the signal distributions in $m_{\rm T}$ and $\Delta\phi(\tau\text{-jet}, \not{E}_{\rm T})$ will be much broader than the background (3), which can distinguish the signal and background events. In Fig. 4 we show the distribution in $\Delta\phi(\tau\text{-jet}, \not{E}_{\rm T})$ for the signal for two values of $m_H = 300\,{\rm GeV}$ and 600 GeV and $\tan\beta = 40$ along with the background. These distributions are for 1 prong τ-jet events passed by the selection cuts: $E_{\rm T}^{\tau\text{-jet}} > 100\,{\rm GeV}$, $R_1 > 0.8$, $\not{E}_{\rm T} > 100\,{\rm GeV}$. In Fig. 5 we show the same distribution in $\Delta\phi(\tau\text{-jet}, \not{E}_{\rm T})$ for τ-jets decaying via 3 prong decay modes. In Figs. 6 and 7 we present the distributions in $m_{\rm T}$ for 1 prong and 3 prong channels of τ-jet, respectively. Evidently, as expected the background is concentrated at small azimuthal opening angle $\Delta\phi \simeq 0$, while the signal is peaked at the largest opening angle, $\Delta\phi \simeq 180^\circ$. Likewise the background distribution in $m_{\rm T}$ is restricted to $m_{\rm T} < m_W$, while the signal distribution is peaked at much larger $m_{\rm T}$ and extends all the way

[3] This is admittedly naive. A more realistic simulation should incorporate the b-tagging efficiency as a function of the kinematic variables. However, we have not incorporated it in our simulation for simplicity and for saving computing time, since it is unrelated to our main concern of tau polarization and tau detection efficiency.

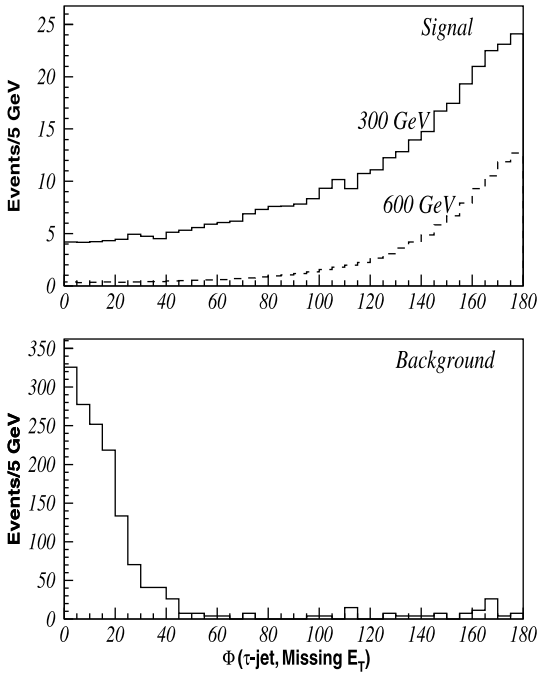

Fig. 4. The number of events are shown against the opening azimuthal angle $\Delta\phi(\tau\text{-jets}, \not{E}_{\mathrm{T}})$ for signal and background for 1 prong decay channel of the τ-jets. These are subject to $p_{\mathrm{T}}^{\tau\text{-jet}} > 100\,\mathrm{GeV}$, $R_1 > 0.8$ and $\not{E}_{\mathrm{T}} > 100\,\mathrm{GeV}$ cuts

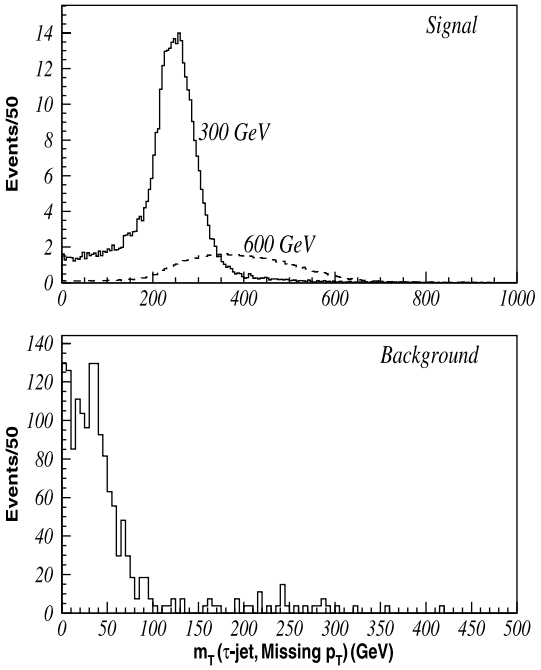

Fig. 6. The number of events are shown against transverse mass m_{T} for signal and background for 1 prong decay channel of the τ-jets. These are subject to $p_{\mathrm{T}}^{\tau\text{-jet}} > 100\,\mathrm{GeV}$, $R_1 > 0.8$ and $\not{E}_{\mathrm{T}} > 100\,\mathrm{GeV}$. The masses of the charged Higgs and $\tan\beta$ are the same as in previous figures

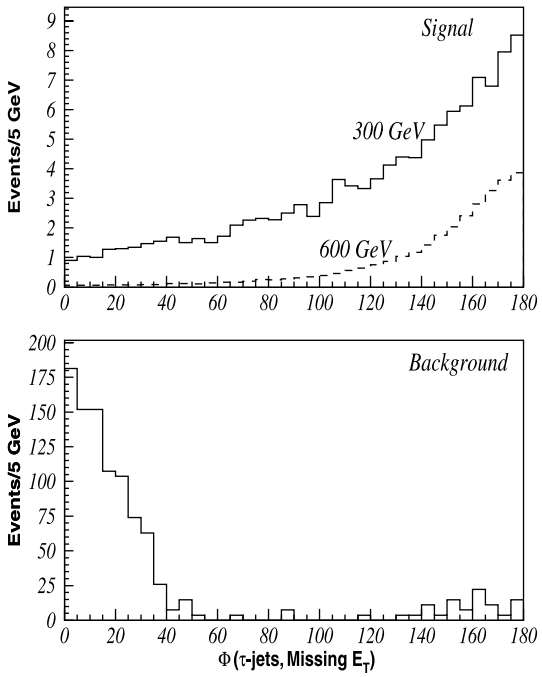

Fig. 5. Same as in Fig. 4, but for the 3 prong decay channel of the τ-jet

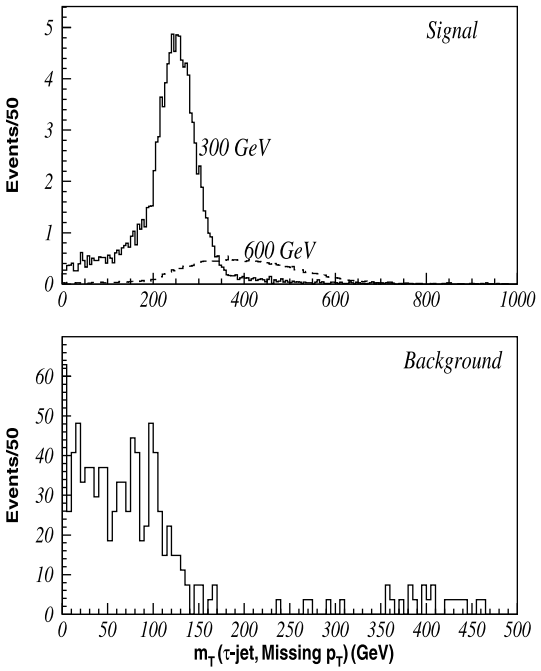

Fig. 7. Same as in Fig. 6, but for the 3 prong decay channel of the τ-jets

up to m_H, which can also be used to estimate the $H^{\pm}$ mass. Thus either a cut on $\Delta\phi$ or m_{T} can suppress the background by enormous amount without practically any loss of signal events. We will see later that a $\Delta\phi > 60^{\circ}$ cut brings down the background level to less than the signal.

In our simulation we have generated 10^6 events each for signal and background processes in the τ + multijet chan-

nel. In Table 1 we demonstrate the cumulative effect of our selection cuts for 1 prong decay channel of the τ-jet, while Table 2 shows the same for 3 prong decay channel of the τ-jet. We present the number of events surviving out of 10^6 generated events after each cut. In both tables we present the results for the signal for the two sets of values of $m_{H^\pm}, \tan\beta = (300\,\text{GeV}, 40)$ and $(600\,\text{GeV},40)$ as well as for the $t\bar{t}$ background. The first row shows the number of hadronically decaying τ particles that come from the $H^\pm$ decay of (2) and the W decay background of (3). It reflects that the hadronic τ decay branching ratio is $\sim 65\%$. The second row shows the number of events having an identified τ-jet, which are subject to the basic cuts of (12)–(14) and where the τ identification is performed using tracker information as discussed above. As expected, the corresponding efficiencies for the signal are higher than the background because of the harder τ-jet from $H^\pm$ decay. For the same reason the efficiency after the $p_{\mathrm{T}}^{\tau\text{-jet}} > 100\,\text{GeV}$ cut, shown in the third row, is about 2.8% for the background, whereas for the signal it is 33% (58%) for $m_H = 300(600)\,\text{GeV}$. In the signal events about three-fourth contribution comes from the 1 prong decay channel and one-fourth contribution is from the 3 prong decay channel of τ, whereas for the background it is 60% from the 1 prong channel and 40% from the 3 prong decay channel of τ. The ratio of signal events in the 1 and 3 prong channels agree with the respective τ branching fractions of 50 and 15%. This shows that the τ identification via the tracker as described above works quite well for the signal events. On the other hand there is a clear excess of 3 prong events in the $t\bar{t}$ background, showing a large contamination of fake τ from hadronic jets in this channel, as mentioned earlier. However, they are removed after the removal of accompanying π^0s via the ΔE cut of (11). After this cut the 3 prong events are about one-fifth of the 1 prong events for both the signal and the background, in

Table 1. Number of events after each set of cuts for two sets of $(M_H, \tan\beta)$ values for the signal and the $t\bar{t}$ background process. The number of τ + multijet events generated in each case is 10^6. The last two rows show the production cross sections in the τ + multijet channel and the cross-section after multiplying with efficiency factors including the b-tagging efficiency for the 1 prong hadronic τ decay channel

Cuts	$m_H, \tan\beta$ (300,40)	$m_H, \tan\beta$ (600,40)	Bg $t\bar{t}$
No. of had. τ decay event	640 531	641 346	641 009
Identified τ jets	448 288	465 556	229 622
$E_{\mathrm{T}}^{\tau\text{-jet}} > 100$ GeV	212 491	370 562	17 875
1 prong decay	158 865	281 428	10 182
$R_{1\pi} > 0.8$	57 240	103 470	1046
$\not{E}_{\mathrm{T}} > 100$ GeV	32 441	89 587	410
Number of jets ≥ 3	15 083	41 783	308
W mass rec, $m_{\mathrm{jj}} = m_W \pm 15$ GeV	9861	27 091	147
Top mass rec, $m_{\mathrm{j}W} = m_t \pm 30$ GeV	6376	17 339	87
$\Delta\phi(\tau\text{-jets}, \not{E}_{\mathrm{T}}) > 60^\circ$	5154	16 394	2
$\sigma \times \mathrm{BR}$ (pb)	0.431	0.045	73
Cross section $\times$ efficiency $\times \epsilon_b$ (fb)	1.1	0.37	0.15

Table 2. Same as in Table 1, but for the τ-jets in the 3 prong decay channel

Cuts	$m_H, \tan\beta$ (300,40)	$m_H, \tan\beta$ (600,40)	Bg $t\bar{t}$
No. of had. τ decay event	640 531	641 346	641 009
Identified τ-jets	448 288	465 556	229 622
$E_{\mathrm{T}}^{\tau\text{-jet}} > 100$ GeV	212 491	370 562	17 875
3 prong decay	53 626	89 134	7683
$\Delta E < 10$ GeV	32 886	54 901	2610
$R_{3\pi} < 0.4$ or > 0.8	18 159	29 714	858
$\not{E}_{\mathrm{T}} > 100$ GeV	10 456	26 173	269
Number of jets ≥ 3	4854	12 161	206
W mass rec, $m_{\mathrm{jj}} = m_W \pm 15$ GeV	3138	7886	110
Top mass rec, $m_{\mathrm{j}W} = m_t \pm 30$ GeV	2010	5073	60
$\Delta\phi(\tau\text{-jets}, \not{E}_{\mathrm{T}}) > 60^\circ$	1676	4881	1
$\sigma \times \mathrm{BR}$ (pb)	0.431	0.045	73
Cross section $\times$ efficiency $\times$ ϵ_b (fb)	0.36	0.11	0.07

agreement with the respective τ branching fractions of 50 and 10%.

The next rows show the effects of τ polarizations on the signal and background. The $R_1 > 0.8$ cut retains about 40% of the signal against only 10% of the background. In fact, the effective loss to the signal is quite small, since the low R_1 peak of Fig. 2 would be lost anyway due to the requirement of a hard charged track for τ identification as mentioned earlier. The corresponding cuts of $R_3 > 0.8$ or < 0.2 retains about 55% of the signal against 35% of the background. It shows the efficacy of τ polarization in the extraction of the $H^{\pm}$ signal in the 1 prong as well as the 3 prong τ-jet channel. Note also that the measurement of the polarization variables R_1 and R_3 is quite simple, since it only requires measuring the momenta of the charged tracks in the tracker.

The $\not{E}_{\mathrm{T}} > 100\,\mathrm{GeV}$ cut has an efficiency of 60(90)% for a $m_{H^{\pm}} = 300(600)\,\mathrm{GeV}$ Higgs signal and 40% for the $t\bar{t}$ background. This is followed by the W and top mass cuts, which have a combined efficiency 20% for the signal as well as the background. Its main utility is in suppressing the $W +$ multijet background, as mentioned earlier. Finally, the $\Delta\phi > 60^{\circ}$ cut suppresses the background by a factor of 50, with very little loss to the signal.

The last but one rows show the signal and background cross-sections in the $\tau +$ multijet channel, representing the 10^6 generated events. It corresponds to $\sigma_{tH^{\pm}} \times \mathrm{BR}(H^{\pm} \to \tau\nu) \times 2/3$ for the signal and $2\sigma_{t\bar{t}} \times 1/9 \times 2/3$ for the background. The last rows show the signal and background cross-sections remaining after all the cuts, which includes a b-tagging efficiency factor of 0.5. We see that at this stage the background is reduced to less than the signal size. It can be still further suppressed via the transverse mass distribution without any loss of signal. The m_{T} distribution can also be used to estimate m_H, as mentioned earlier. Thus, the discovery limit is primarily controlled by the size of the signal shown in the last row. Figure 8 shows the discovery limit corresponding to 25 signal events for the 1 prong and $(1+3)$ prong channel of the τ-jet. This is shown separately for $\mathcal{L} = 30\,\mathrm{fb}^{-1}$ and $100\,\mathrm{fb}^{-1}$ expected from the low and high luminosity runs of LHC separately. It shows a promising discovery potential for $H^{\pm}$ over the mass range up to 600–700 GeV at moderate to large $\tan\beta$. However, it should be noted here that a full simulation for the high luminosity run has not been completed yet [21]. It would require a higher trigger threshold of the τ-jets, which would move up the discovery limits at low m_H to slightly higher values of $\tan\beta$.

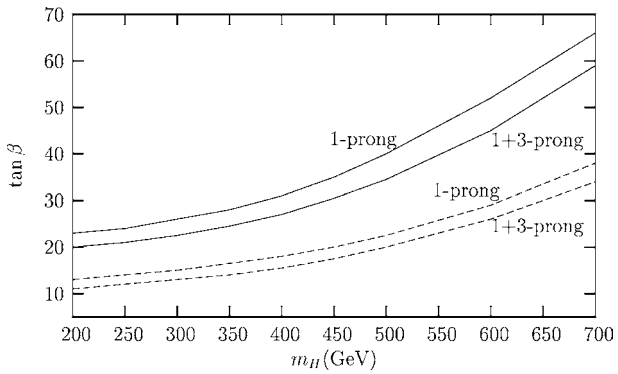

Fig. 8. Discovery limits of charged Higgs are shown as functions of $\tan\beta$ for an integrated luminosity $\mathcal{L} = 30\,\mathrm{fb}^{-1}$ (*solid lines*) and $\mathcal{L} = 100\,\mathrm{fb}^{-1}$ (*dashed lines*) for $H^{\pm} \to \tau\nu$, where τ decays hadronically in both the 1 prong and 3 prong channel. In each case the contribution from the 1 prong channel only are shown by *upper lines*, whereas the contribution from the combined 1 and 3 prong channels are shown by *lower lines*

4 Summary

We have investigated the $H^{\pm}$ signal at LHC in the 1 and 3 prong hadronic τ-jet channels along with the $t\bar{t}$ background. The signal and background processes were generated using the PYTHIA event generator interfaced with TAUOLA for the 1 and 3 prong hadronic τ decays. The detector response was simulated using the fast simulation packages CMSJET. We have shown that the opposite polarization of τ from the signal ($H^{\pm} \to \tau\nu$) and background ($W^{\pm} \to \tau\nu$) processes can be effectively used to suppress the background with respect to the signal in both the 1 and 3 prong τ-jet channels. The signal was also found to have much harder distributions than the background in the azimuthal opening angle ($\Delta\phi$) between the τ-jet and the missing E_{T} as well as in the transverse mass (m_{T}) of the two. Combining these distinctive features with those of τ polarization we could effectively suppress the background to below the signal size. Thus the $H^{\pm}$ discovery potential of LHC in the 1 and 3 prong τ-jet channels is primarily determined by the signal cross-section in these channels. We find a promising $H^{\pm}$ signal at LHC over the mass range of several hundred GeV at moderate to large $\tan\beta$.

Acknowledgements. One of the authors (D.P.R.) acknowledges partial financial support from BRNS (DAE) through the Raja Ramanna Fellowship scheme.

References

1. D.P. Roy, Mod. Phys. Lett. A **19**, 1813 (2004)
2. D.P. Roy, Phys. Lett. B **459**, 607 (1999)
3. S. Eidelman et al., Phys. Lett. B **592**, 1 (2004)
4. R. Kinnunen, CMS note 2000/045
5. CMS Physics Technical Design Report, CERN/LHCC 2006/021
6. R. Kinnunen, CMS Note 2006/100
7. T. Sjostrand, P. Eden, C. Friberg, L. Lonnblad, G. Miu, S. Mrenna, E. Norrbin, Comput. Phys. Commun. **135**, 238 (2001)
8. S. Abdullin, A. Khanov, N. Stepanov, CMS Note 1994/180
9. K.A. Assamagan, Y. Coadou, A. Deandrea, Eur. Phys. J. C **4**, 9 (2002)
10. S. Jadach, Z. Was, R. Decker, J.H. Kuehn, Comput. Phys. Commun. **76**, 361 (1993)
11. P. Golonka et al., hep-ph/0312240 and references therein

12. S.H. Zhu, Phys. Rev. D **67**, 075 006 (2003)
13. T. Plehn, Phys. Rev. D **67**, 014 018 (2003)
14. E.L. Berger, T. Han, J. Jiang, T. Plehn, Phys. Rev. D **71**, 115 012 (2005)
15. N. Kidonakis, hep-ph/0511235
16. J. Alwall, J. Rathsman, JHEP **0412**, 050 (2004)
17. N. Kidonakis, R. Vogt, Phys. Rev. D **68**, 114 014 (2003)
18. CDF collaboration, F. Abe et al., Phys. Rev. Lett. **79**, 3585 (1997)
19. A. Abulencia et al., Phys. Rev. Lett. **96**, 011 802 (2006)
20. R. Kinnunen, A. Nikitenko, CMS Note 2003/006
21. S. Gennai et al., CMS note 2006/028